Bioorganic Chemistry 89 (2019) 102986

Contents lists available at ScienceDirect

Bioorganic Chemistry

journal homepage: www.elsevier.com/locate/bioorg

Targeting malaria and leishmaniasis: Synthesis and pharmacological evaluation of novel pyrazole-1,3,4-oxadiazole hybrids. Part II

Garima Verma[a], Mohemmed Faraz Khan[a], Lalit Mohan Nainwal[a], Mohd Ishaq[b], Mymoona Akhter[a], Afroz Bakht[c], Tariq Anwer[d], Farhat Afrin[e], Mohammad Islamuddin[f], Ibraheem Husain[f], Mohammad Mumtaz Alam[a,*], Mohammad Shaquiquzzaman[a,*]

[a] Department of Pharmaceutical Chemistry, School of Pharmaceutical Education and Research, Jamia Hamdard, New Delhi 110062, India
[b] Department of Pharmacology, School of Pharmaceutical Education and Research, Jamia Hamdard, New Delhi 110062, India
[c] Department of Chemistry, College of Science and Humanities, Prince Sattam Bin Abdulaziz University, P.O. Box-173, Al-Kharj, Saudi Arabia
[d] Department of Pharmacology, College of Pharmacy, Jazan University, P.O. Box 114, Gizan, Saudi Arabia
[e] Department of Medical Laboratory Technology, Faculty of Applied Medical Sciences, Taibah University, Madina, Saudi Arabia
[f] Molecular Virology Lab, Centre for Interdisciplinary Research in Basic Sciences, Jamia Millia Islamia University, New Delhi, India

ARTICLE INFO

Keywords:
Pyrazole-4-acrylic acid
1,3,4-Oxadiazole
Antimalarial
Antileishmanial
Falcipain-2

ABSTRACT

In continuance with earlier reported work, an extension has been carried out by the same research group. Mulling over the ongoing condition of resistance to existing antimalarial agents, we had reported synthesis and antimalarial activity of certain pyrazole-1,3,4-oxadiazole hybrid compounds. Bearing previous results in mind, our research group ideated to design and synthesize some more derivatives with varied substitutions of acetophenone and hydrazide. Following this, derivatives **5a–r** were synthesized and tested for antimalarial efficacy by schizont maturation inhibition assay. Further, depending on the literature support and results of our previous series, certain potent compounds (**5f**, **5n** and **5r**) were subjected to Falcipain-2 inhibitory assay. Results obtained for these particular compounds further strengthened our hypothesis. Here, in this series, compound **5f** having unsubstituted acetophenone part and a furan moiety linked to oxadiazole ring emerged as the most potent compound and results were found to be comparable to that of the most potent compound (indole bearing) of previous series. Additionally, depending on the available literature, compounds (**5a–r**) were tested for their antileishmanial potential. Compounds **5a, 5c** and **5r** demonstrated dose-dependent killing of the promastigotes. Their IC_{50} values were found to be 33.3 ± 1.68, 40.1 ± 1.0 and 19.0 ± 1.47 μg/mL respectively. These compounds (**5a, 5c** and **5r**) also had effects on amastigote infectivity with IC_{50} of 44.2 ± 2.72, 66.8 ± 2.05 and 73.1 ± 1.69 μg/mL respectively. Further target validation was done using molecular docking studies. Acute oral toxicity studies for most active compounds were also performed.

1. Introduction

Malaria is considered as the most threatening parasitic infection in humans and has been a matter of concern for centuries [1]. As per the World Malaria Report, 2016 by WHO, around 429,000 deaths occurred due to malaria globally. Majority of the deaths were reported in WHO African region, particularly in the Sub-Saharan Africa. *Plasmodium falciparum* (*P. falciparum*) was found to be responsible for majority of the deaths. 303,000 deaths (equivalent to 70% of the global total are estimated to have occurred in children under five years of age [2].

Considering such an alarming condition of spread of these menaces and the datum of emergence of resistance to the available antimalarial agents, our research group had previously envisioned to develop novel antimalarials. So, a series of pyrazole-1,3,4-oxadiazole based compounds targeting malaria was previously synthesized and reported [3]. Amongst compounds of the preceding series, compound **6v** (Fig. 1) was the most active one (against both chloroquine sensitive and resistant strains of *P. falciparum*) having unsubstituted acetophenone part connected to pyrazole and a heteroaromatic ring (indole) linked to oxadiazole. From results, it was inferred that the presence of unsubstituted acetophenone part along with a heteroaromatic ring attached to oxadiazole moiety greatly favored antimalarial effects.

From results of the previous study, it was found that amide derivatives elicited promising anticancer effects whereas oxadiazole

* Corresponding author.
E-mail addresses: drmmalam@gmail.com (M.M. Alam), shaqiq@gmail.com (M. Shaquiquzzaman).

https://doi.org/10.1016/j.bioorg.2019.102986
Received 25 December 2018; Received in revised form 6 April 2019; Accepted 16 May 2019
Available online 17 May 2019

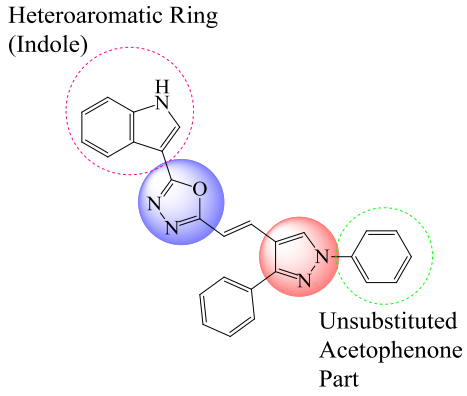

Fig. 1. Most Active Compound of previously reported Series.

derivatives emerged as potent antimalarial agents.

On the other hand, leishmaniasis continues to prevail in the list of neglected tropical diseases. This malevolent infectious disease is known to be caused by intramacrophage protozoa of the genus *Leishmania*. Amongst the various known forms of leishmaniasis, visceral, cutaneous and mucocutaneous, visceral form is the most fatal one. *Leishmania donovani* (*L. donovani*) is the causative organism behind this form of disease while this gets transmitted by the bite of phlebotomine sand flies [4,5]. Countries like India, Brazil, South Sudan, Ethiopia and Bangladesh contribute to the 90% global burden of this disease. Despite availability of a number of treatment options, there is a pressing need for the development of novel, effective, cost effective and better patient compliant treatment options to curb this menace. Toxicity, long duration of treatment, high cost of treatment and parasitic resistance are the problems associated with the current therapeutic regimen [6].

Literature gives strong evidences regarding antileishmanial activity of pyrazole based compounds (Fig. 2). Compound **I** synthesized by Santos and group demonstrated very promising effects against *Leishmania amazonensis* (*L. amazonensis*) with an IC_{50} value of 15.5 ± 6.8 μM [7]. Faria et al. determined antileishmanial potential of pyrazole based carbonitriles and its derivatives and reported compound **II** as the most potent candidate against *Leishmania braziliensis* (*L. braziliensis*) with an IC_{50} value of 15 ± 0.14 μM [8]. Certain pyrazole derivatives were developed and screened for antileishmanial activity by Taha et al. Amongst those synthesized compounds, compound **III** was highly active with IC_{50} value of 0.0112 μg/mL when tested against *L. donovani* [9]. Amongst a series of pyrazole based compounds prepared and evaluated by Bekhit and co-workers, compound **IV** exhibited maximum activity with IC_{50} value of 0.13 ± 0.02 μg/mL against *Leishmania aethiopica* (*L. aethiopica*) [10].

Antileishmanial activity of oxadiazole based compounds is also well documented in the literature. Phenyl linked oxadiazole-phenylhydrazone hybrids synthesized by Taha et al. were assessed for antileishmanial potential. The group reported compound **V** as the most potential candidate with an IC_{50} value of 0.95 ± 0.01 μM [11]. In another series of quinolinyl-oxadiazole hybrids reported by Taha and group, compound **VI** emerged as the most potent agent with IC_{50} value of 0.10 ± 0.001 μM [12] (Fig. 3).

Incited by promising results of the previous series, we synthesized another series of compounds (Scheme 1) bearing pyrazole and 1,3,4-oxadiazole with differently substituted acetophenones and hydrazides (**5a–r**). These derivatives were tested for evaluated for both antimalarial and antileishmanial efficacy. Previously, promising antimalarial results were obtained for 1,3,4-oxadiazole derivatives. Since, leishmaniasis is also one of the protozoal diseases, it was envisaged to assess antileishmanial efficacy for these compounds. Available literature in this context also gave substantial support.

2. Results & discussion

2.1. Chemistry

Desired compounds were obtained *via* different reaction steps mentioned in Scheme 1. Substituted acetophenone derivatives reacted with phenylhydrazine leading to the formation of corresponding hydrazone derivatives involving addition reaction. Further, Vilsmeir-Haack reaction was used involving formylation of the aromatic compounds using *N-N*-dimethyl formamide (DMF) as an acylating agent in the presence of activating agent ($POCl_3$) [13]. After this, acrylic acid derivatives were synthesized by treatment of pyrazole carbaldehydes with malonic acid in the presence of pyridine and piperidine. Mechanism for formation of the acrylic acid derivatives involved Knoevenagel condensation followed by Doebner modification [14,15].

Finally, the prepared acrylic acid derivatives reacted with substituted benzohydrazide derivatives and lead to the formation of desired 1,3,4-oxadiazole derivatives in the presence of $POCl_3$. Synthesized derivatives have been listed in Table 4.

2.1.1. Spectral characterization

Formation of the desired 1,3,4-oxadiazole derivatives was supported by spectral and analytical data. For α,β-unsaturated carboxylic acid derivatives (**2a–c**), characteristic acidic peak was observed in the region of 12.31 to 12.33 ppm in ^{1}HNMR spectra.

Trans conformation of acrylic protons (CH=CH) was observed using ^{1}H NMR spectra (**2a–c**). *J* value was found to be in the range of 15.6–16.4 Hz, thereby confirming existence of *trans* conformation. α and β protons were observed in the range of 6.39–6.94 and 7.40–7.68 ppm respectively. Pyrazole proton appeared as a singlet (*s*) in the region of 8.27–9.12 ppm.

Further evidence in the support of formation of 1,3,4-oxadaizole derivatives was obtained from ^{13}C NMR, IR and mass spectral data

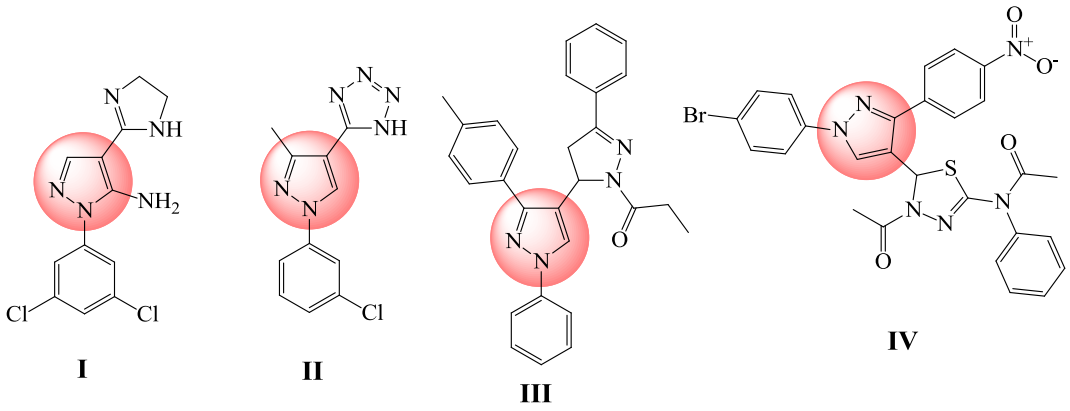

Fig. 2. Pyrazole based Antileishmanial Compounds.

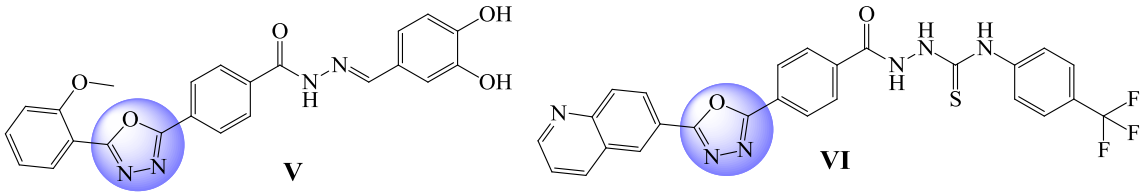

Fig. 3. 1,3,4-Oxadiazole based Antileishmanial Agents.

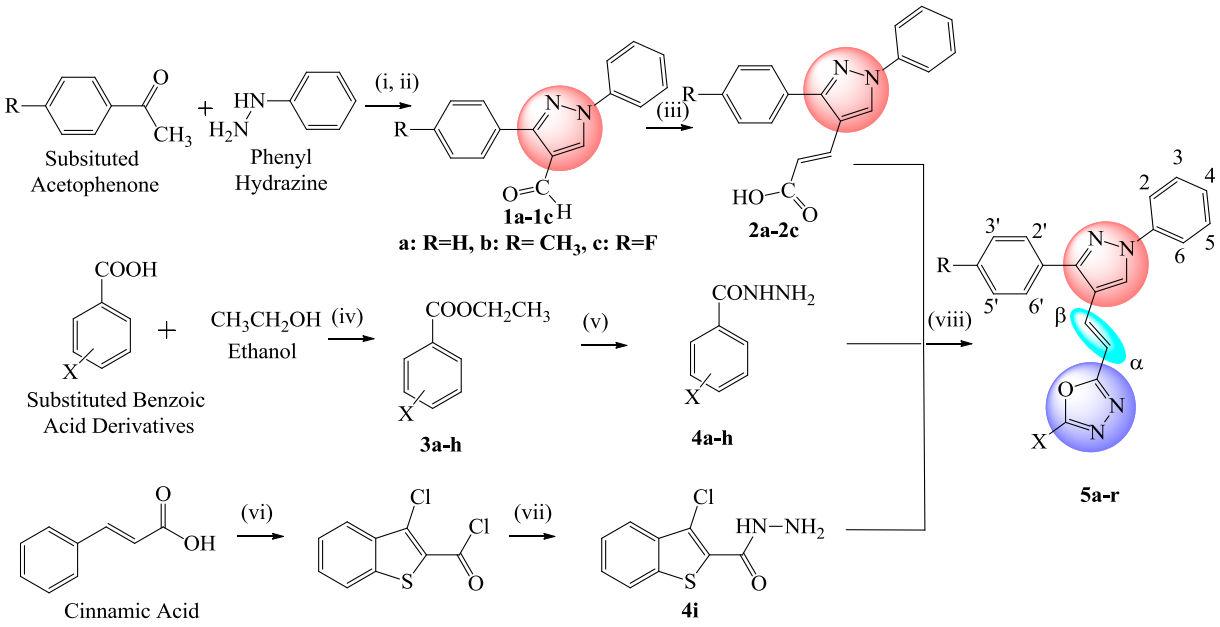

Scheme 1. Reagents and conditions: (i, ii) Glacial acetic acid, methanol, refulx, dimethyl formamide, phosphorus oxyhloride; (iii) Malonic acid, pyridine, reflux; (iv) Conc. H_2SO_4, reflux; (v) Hydrazine hydrate, reflux; (vi) $SOCL_2$ DMF, Pyridine; (vii) Hydrazine hydrate, reflux (vii) phosphorus oxychloride, stirring, heating (60–70 °C).

(**5a–r**). Peaks in the region of 161–164 ppm in ^{13}C NMR spectra gave a confirmation for oxadiazole formation. IR spectral data also supported the formation of proposed oxadiazole derivatives. Characteristic peaks for C═N, C═C and C−O−C were observed at their expected values.

Experimental and calculated values of elemental analysis were in consonance with each other. Results were found to be well within range of ± 0.4% of theoretical values. Mass spectral data further confirmed the formation of desired compounds. Isotopic peaks were seen in case of chloro bearing compounds *i.e.* **5l**, **5m** and **5r**. In **5l** and **5m**, owing the presence of dichloro groups, $[M+H]^+$, $[M-2+H]^+$ and $[M-4+H]^+$ peaks were observed. However, in case of **5r** (mono chloro substituted) $[M+H]^+$ and $[M-2+H]^+$ peaks were observed.

2.2. Pharmacological activity

2.2.1. Antimalarial activity

2.2.1.1. Schizont maturation inhibition assay. Schizont maturation inhibition assay was employed for evaluating *in vitro* antimalarial activity of the synthesized compounds (**5a–r**). Activity was done using a culture of 3D7 strain of *P. falciparum*. Following confirmation of schizont maturation, blood smears were prepared. These prepared slides were examined under microscope. Total number of schizonts per 200 parasites was calculated. Following this, IC_{50} value for all the compounds was determined (Table 1). On evaluation, compound **5f** emerged as the most potent compound with IC_{50} value of 0.248 μg/mL against 3D7 strain. Certain other compounds of the series (**5n**, **5r**, **5o**, **5g** and **5a**) displayed promising antimalarial effects with IC_{50} value of less than 1.0 μg/mL. Results obtained for this particular set of compounds were quite comparable to the previously reported compounds [3].

Table 1
Antimalarial effects (IC_{50} CQ Sensitive: 3D7 strain of *P. falciparum*) of compounds **5a–r.**

S. No.	Compd.	IC_{50} CQ Sensitive (μg/mL)	S. No.	Compd.	IC_{50} CQ Sensitive (μg/mL)
1.	**5a**	0.886	**2.**	**5b**	1.708
3.	**5c**	1.180	**4.**	**5d**	2.234
5.	**5e**	2.203	**6.**	**5f**	0.248
7.	**5g**	0.647	**8.**	**5h**	2.302
9.	**5i**	2.736	**10.**	**5j**	1.650
11.	**5k**	2.769	**12.**	**5l**	3.073
13.	**5m**	4.316	**14.**	**5n**	0.322
15.	**5o**	0.582	**16.**	**5p**	1.942
17.	**5q**	3.382	**18.**	**5r**	0.494
19.	**Chloroquine**	0.405			

CQ: Chloroquine.

Antimalarial effects of compound **5f** (IC_{50} = 0.248 μg/mL) can be visualized from Fig. 4. Fig. 4a represents the view taken from microscope for control well. In this figure, a number of schizonts can be seen (bright violet dots/cluster of dots present over the background of RBCs). In the view taken for compound **5f**, schizonts are not visible (Fig. 4b). In this microscopic view, a clear background of stained RBCs can be seen. For this study, chloroquine was taken as the standard agent.

A few compounds (**5a, 5f, 5g, 5n, 5o** and **5r)** showed promising antimalarial effects with IC_{50} value of less than 1 μg/mL against chloroquine sensitive strain. These compounds were also evaluated against the chloroquine resistant strain (RKL 9) of the parasite. Further, in order to assess toxicity of these compounds, *in vitro* cytotoxicity

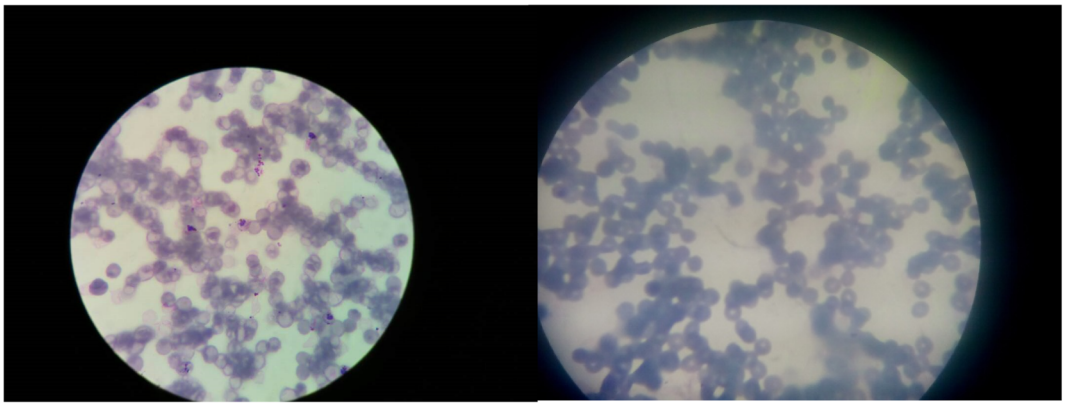

Fig. 4. (a) Control Well; **(b):** Antimalarial Effects of Compound.

Table 2
Selectivity Index and IC_{50} (CQ Resistant: RKL 9 strain of *P. falciparum* and Falcipain-2 Inhibition) of Compounds.

S. No.	Compd.	SI	IC_{50} CQ resistant (μg/mL)	Resistance index	IC_{50} (Falcipain-2) (μM)
1.	**5a**	29.1	2.129	2.40	ND
2.	**5f**	13.4	0.863	3.47	14
3.	**5g**	27.3	2.025	3.12	ND
4.	**5n**	22.5	0.882	2.73	21
5.	**5o**	17.6	1.705	2.92	ND
6.	**5r**	19.2	1.659	3.35	110
7.	**Chloroquine**	–	2.154	5.31	–
8.	**DMSO**	–	–	–	0
9.	**E64**	–	–	–	0.02

ND: Not Determined; SI: Selectivity Index.

evaluation was performed using *Vero* cell line. Their Selectivity Index (SI) was also determined (Table 2).

2.2.1.2. Falcipain-2 assay. For target identification, further screening for inhibitory activity against recombinant Falcipain-2 using Cbz-Phe-Arg-AMC (fluorogenic substrate) was carried out for compounds, **5a**, **5f**, **5g, 5n, 5o** and **5r**. An equivalent concentration of DMSO served as the negative control whereas E64 served the purpose of positive control. This assay was performed at concentrations of 100, 50 and 25 μM (Table 2). Falcipain-2 inhibitory activity was assessed by cleavage of the fluorogenic substrate, releasing the fluorescent AMC group. A decrease in the fluorescence intensity of the sample was indicative of inhibition of enzyme activity. Compounds which showed more than 50% inhibition at a concentration of 25 μM were taken for IC_{50} value determination. Compound **5f** was the most potent inhibitor of Falcipain-2 with an IC_{50} value of 14 μM.

2.2.1.3. Molecular docking studies. An effort for identification of novel and potential antimalarial agents has been made in the present study. Further, in order to determine their probable mode of action, docking studies were done against falcipain-2 enzyme. Glide score for the most active compound was found to be −5.532. Dock pose and two dimensional ligand interaction diagram for the same is presented as Fig. 5a and 5b respectively.

Dock pose for compound **5f** with catalytic domain of falcipain-2 (PDB ID: **1YVB**) is represented in Fig. 5a. 2D ligand interaction diagram for the same is given in Fig. 5b. Formation of hydrogen bond between one of the nitrogen atoms of the oxadiazole ring and side chain of protein (HIP 159) is clearly evident from Fig. 5b. This bond is shown in the figure as purple dotted arrow. For better understanding of the interactions, different interactions along with their color coding have been shown in Fig. 5c. Polar amino acid residues, represented in cyan color, found responsible for interaction were Ser 29, Asn 64, Asn 21, Gln 19, Asn 158, Ser 24, Ser 133, Asn 69 and Gln 156. Interactions were also observed between the compound and certain non polar amino acid residues (green color) like Cys 63, Ala 160, Cys 22, Trp 177, Val 136, Cys 25, Trp 26, Ile 132, Phe 207, Leu 67, Ile 68, Leu 157 and Val 134. Positively charged amino acid residues (blue color) having interactions with **5f** were Lys 20 and Hip 159. One negatively charged residue (red color), Asp 205 showed interaction with the compound. Compound **5f** also interacted with Gly 65, Gly 23 and Gly 66, represented in golden color. Apart from all these interactions, significant solvent exposure was seen in the region of furan, 1,3,4-oxadiazole, biphenyl ring systems attached to pyrazole. This solvent exposure was thought to promote the interactions between our compound and the protein.

2.2.2. Antileishmanial activity

2.2.2.1. Initial Screening of compounds. Synthesized compounds were tested for antileishmanial activity as well against *L. donovani* (MHOM/IN/83/AG83) promastigotes. Parasites were treated with compounds at a concentration of 100 μg/mL. Viability of compounds was determined under phase contrast microscope (400×). It was observed that compounds **5a, 5c** and **5r** exhibited significant inhibitory effects against promastigotes. However, other tested compounds did not show significant inhibition (Fig. 6).

2.2.2.2. Determination of IC_{50} of compounds against promastigotes. MTT reduction assay was used for evaluating the antileishmanial activity of compounds against *L. donovani* promastigotes. Compounds **5a, 5c** and **5r** (0–100 μg/mL) demonstrated dose-dependent killing of the promastigotes. Their IC_{50} values were found to be 33.3 ± 1.68, 40.1 ± 1.0 and 19.0 ± 1.47 μg/mL respectively (Fig. 7). Established antileishmanial drug, Pentamidine was taken as positive drug control. This drug showed a similar trend in dose dependent parasite killing with IC_{50} value of 2.6 ± 0.32 μg/mL. Parasite viability was not affected by the presence of negative control, DMSO (0.2%).

2.2.2.3. Antileishmanial effect of compounds against intracellular amastigotes. Activity of compounds **5a, 5c** and **5r** on internalized amastigotes was determined microscopically on Giemsa-stained macrophages. Macrophages entry by promastigotes involves the formation of membrane bound parasitophorous vacuoles, where they get transformed into nonmotile amastigote form. Survival of parasites within the parasitophorous vacuoles is an indicator of pathogenesis. Thereby, it was important to determine activity of **5a, 5c** and **5r** against the macrophage resident amastigotes. Results depicted a dose-dependent inhibition of **5a, 5c** and **5r** compounds (0–100 μg/mL) on amastigote infectivity with IC_{50} of 44.2 ± 2.72, 66.8 ± 2.05 and 73.1 ± 1.69 μg/mL respectively (Fig. 8).

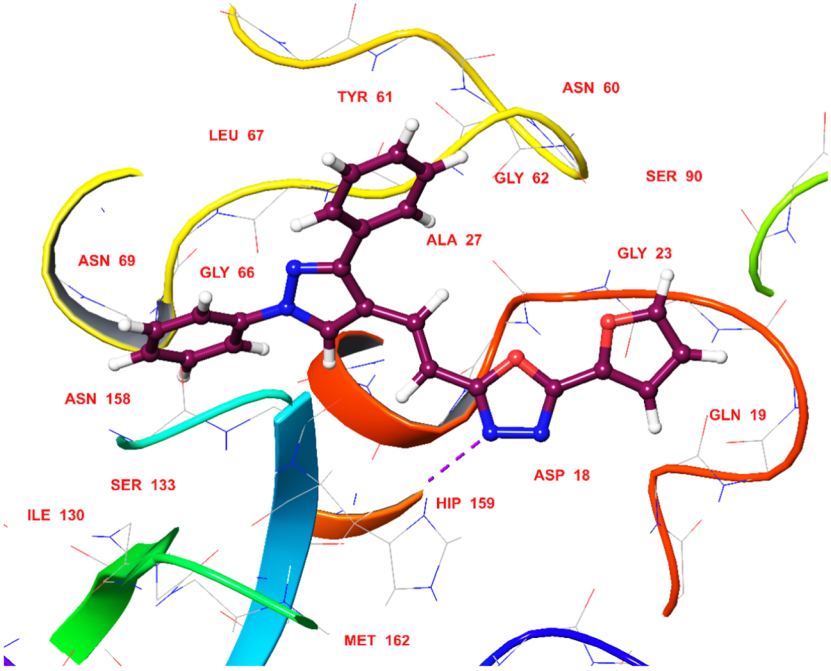

(a)

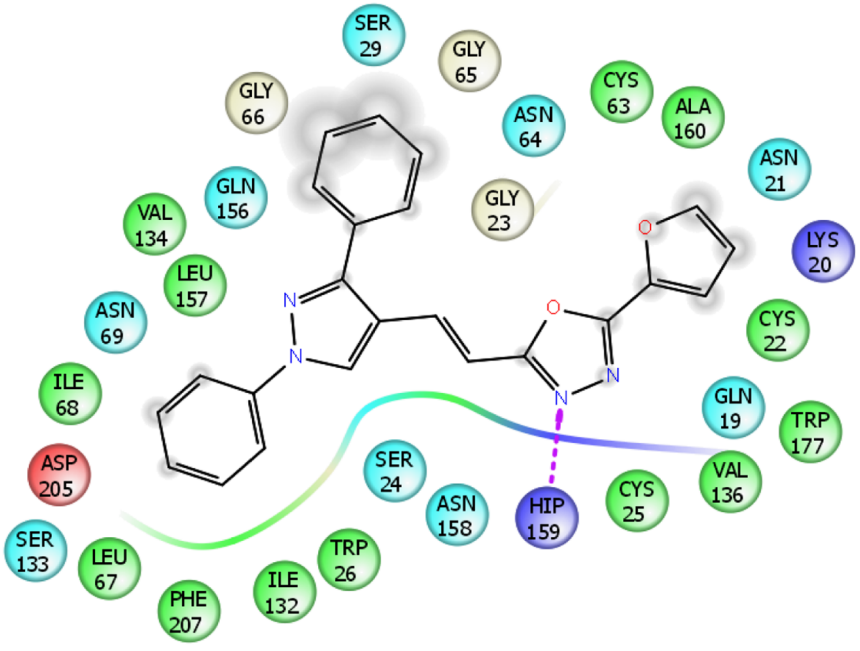

(b)

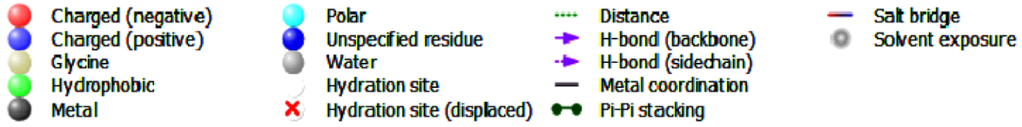

(c)

Fig. 5. (**a**). Dock Pose of Compound **5f** with **1YVB**; (**b**): Ligand Interaction Diagram of Compound **5f** with Ligand Binding Domain of Falcipain 2 (**1YVB**); (**c**) Legends for Interactions.

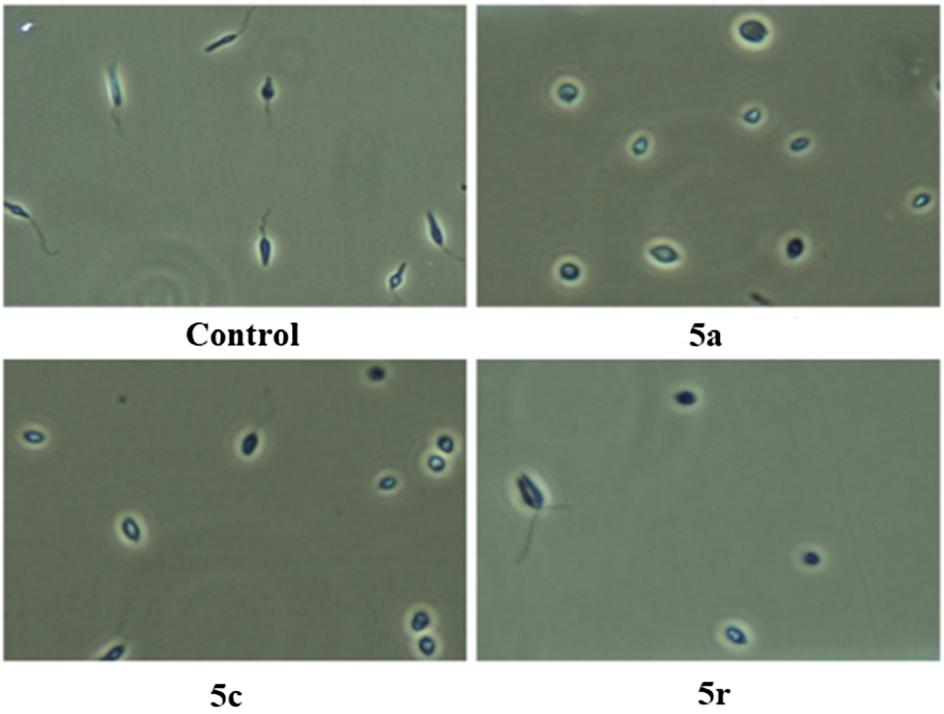

Fig. 6. Screening of compounds. Exponential-phase *L. donovani* promastigotes (2×10^6 cells/mL) were incubated with 100 μg/mL of synthesized compounds for 48 h and analyzed by light microscopy (400× magnification).

2.2.2.4. Cytotoxicity of the test compounds on RAW264.7 Macrophage. In vitro cytotoxicity assay was carried out with the murine macrophage cell line RAW264.7 to determine the adverse effects of **5a, 5c** and **5r**, using Pentamidine as a reference drug. The toxicity assay showed that compounds **5a, 5c** and **5r** had no significant adverse effects on the viability and morphology of the macrophages (Fig. 9).

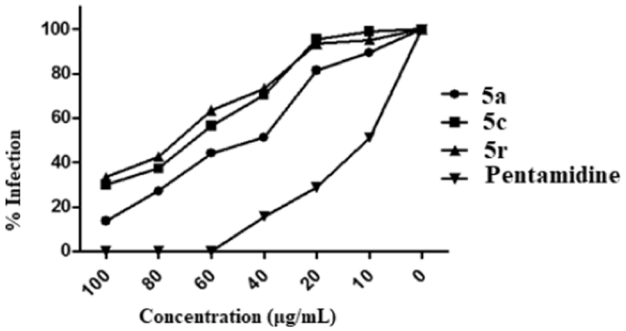

Fig. 8. Promastigote-infested RAW264.7 macrophages were incubated at 37 °C in CO_2 incubator with compounds **5a, 5c** and **5r** (0–100 μg/mL) for 48 h at 37 °C. % infectivity estimated for determination of IC_{50} on amastigotes (inset). Each point corresponds to the mean of triplicate samples and is representative of one of three independent experiments.

2.3. Acute oral toxicity studies

OECD guidelines were followed for carrying out acute oral toxicity studies. Dose used in these studies was 300 mg/Kg. For toxicity evaluation, histopathological evaluation along with biochemical testing were done. General behavior and appearance of the rats were observed initially during first 30 min of dosing, at an interval of 6 h, 14 h and thereafter, regularly for a period of 14 days for compounds **5f** and **5r**. In both control and test groups, rats appeared completely normal, both in terms of appearance and behavior. All the

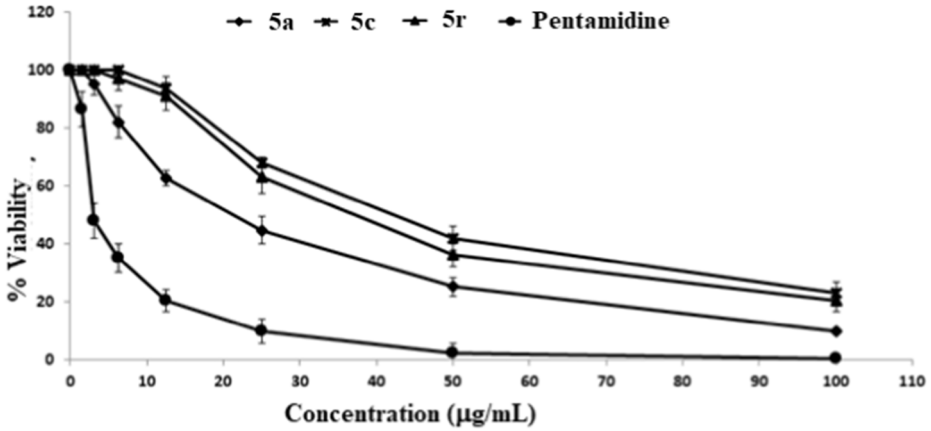

Fig. 7. Log phase *Leishmania donovani* promastigotes were incubated with compounds **5a, 5c** and **5r** (0–100 μg/mL) for 48 h at 22 °C for IC_{50} determination. Each point or bar corresponds to the mean of triplicate samples and is representative of one of three independent experiments.

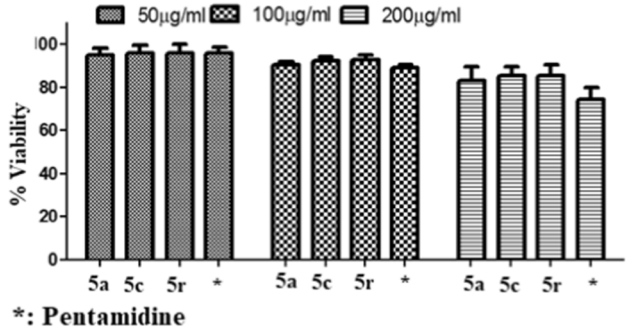

Fig. 9. Cytotoxicity of compounds **5a, 5c** and **5r** to RAW 264.7 macrophages ascertained as % viability 48 h post-incubation with increasing concentrations of **5a, 5c** and **5r** or Pentamidine (50, 100 and 200 mg/mL). Each point corresponds to the mean ± SE of triplicate samples and is representative of one of three independent experiments.

Table 3
Parameters observed.

Observation	Control				Compounds **5f** and **5r**			
	30 min	6 h	14 h	Till 14th Day	30 min	6 h	14 h	Till 14th Day
Skin and Fur	N	N	N	N	N	N	N	N
Eyes	N	N	N	N	N	N	N	N
Mucous Membrane	N	N	N	N	N	N	N	N
Behavioral Pattern	N	N	N	N	N	N	N	N
Salivation	N	N	N	N	N	N	N	N
Lethargy	N.O.	N.O.	N.O.	N.O.	N.O.	N.O.	N.O.	N.O.
Sleep	N	N	N	N	N	N	N	N
Diarrhea	N.O.	N.O.	N.O.	N.O.	N.O.	N.O.	N.O.	N.O.
Coma	N.O.	N.O.	N.O.	N.O.	N.O.	N.O.	N.O.	N.O.
Tremors	N.O.	N.O.	N.O.	N.O.	N.O.	N.O.	N.O.	N.O.

N: Normal.
N.O.: Not Observed.

parameters observed during the observation period have been tabulated in Table 3.

Following an observation period of 14 days, all the animals were sacrificed on 15th day. Liver tissue of all the animals was excised. Slides were prepared using this tissue to examine histopathological changes, if any. Liver sections of control and test group are shown in Fig. 10a and 10b for **5f** and **10c** and **10d** for **5r** respectively. In the microscopic view of slides, architecture of both the groups appeared normal, showing no evidences of toxicity.

For carrying out biochemical estimation of both the groups, blood was collected from rats, plasma portion was separated and sent for evaluation. Three tests, namely liver function test (LFT), kidney function test (KFT) and lipid profile were performed. Results of all the three tests suggested no signs of toxicity. Values for all the tested parameters lied well within the normal prescribed range (Fig. 11).

3. Experimental

3.1. Chemistry

All the chemicals required for synthesis of the desired compounds were obtained from commercial suppliers and were utilized without any further purification. For thin layer chromatography (TLC), aluminum backed silica plates (Merck, silica gel 60 F254) were used. Melting points were taken using pen capillaries and are uncorrected. Bruker alpha-T spectrophotometer was used for recording infra-red (IR) spectra. ^{1}H and ^{13}C nuclear magnetic resonance (NMR) spectra were recorded on Bruker Avance-400 (400 and 100 MHz, respectively). Tetramethylsilane (TMS) was as an internal standard for recording NMR spectra. $CDCl_3$ and DMSO were used as NMR solvents. Chemical shift values (δ) and coupling constants (J) have been reported in parts per million (ppm) and Hertz (Hz) respectively. Perkin-Elmer model 240 was used for elemental analyses. Yields refer to products obtained after crystallization.

Desired compounds were synthesized in accordance with the steps mentioned in Scheme 1. Substitutions for all the synthesized derivatives are given in Table 4.

3.1.1. General procedure to synthesize 1,3-Diphenyl-1H-pyrazole-4-carbaldehyde (1a–c)

Dimethyl formamide (DMF) and phosphorus oxychloride ($POCl_3$) were separately cooled down to a temperature of 0 °C. To previously cooled DMF (0.075 mol) at 0–5 °C, $POCl_3$ was added drop-wise through dropping funnel. The resulting solution was stirred for 15 min. A solution of hydrazone (prepared by refluxing desired acetophenone in methanol in the presence of catalytic amount of glacial acetic acid), made using minimum quantity of DMF was added to the mixture in drop-wise manner. The resulting mixture was warmed to room temperature and subsequently heated to a temperature of 75–80 °C for a period of 5 hrs. Completion of the reaction was judged using TLC. Following completion, reaction mixture was cooled to room temperature and basified using a saturated solution of $NaHCO_3$. Precipitate obtained on basification was filtered, washed and dried [16,17].

3.1.2. General procedure to synthesize 3-(1,3-diphenyl-1H-pyrazol-4-yl) acrylic acid derivatives (2a–c)

Pyrazole-4-carbaldehyde derivatives (0.01 mol) were dissolved in pyridine (10 mL). To this solution, malonic acid (0.05 mol) and piperidine in catalytic amount (0.5 mL) were added. The resulting mixture was stirred for a period of 8 hrs. After stirring, the mixture was heated to a temperature of 95–100 °C. Progress of the reaction was determined using TLC. Following completion, processing for the reaction was done. The reaction mixture was poured on to crushed ice followed by basification using NaOH solution. Further acidification using dilute HCl gave the desired acid derivatives.

*3.1.2.1. 3-(1,3-diphenyl-1H-pyrazol-4-yl)acrylic acid (**2a**).* Yield (%): 89; Appearance: White powder; m.p. 184–186 °C; IR (cm^{-1}): 1684 (C═O); ^{1}H NMR (400 MHz, DMSO): 6.41 (d, 1H, *H*-α, J = 15.6), 7.35 (t, 1H, H-4, J = 7.2), 7.46–7.62 (m, 8H, H-β, 2,3,5,6,3′,4′,5′), 7.90 (d, 2H, H-2′,6′, J = 8.0), 9.21 (s, 1H, *H*-Pyrazole), 12.33 (s, 1H, −COOH); Elemental analysis (%) of $C_{18}H_{14}N_2O_2$, calculated/found: C (74.45/74.47), H (4.89/4.86), N (9.62/9.65).

*3.1.2.2. 3-(1-phenyl-3-(p-tolyl)-1H-pyrazol-4-yl)acrylic acid (**2b**).* Yield (%): 87; Appearance: White powder; m.p. 194–196 °C; IR (cm^{-1}): 1688 (C═O); ^{1}H NMR (400 MHz, DMSO): 6.39 (d, 1H, *H*-α, J = 15.6), 7.33–7.37 (m, 3H, H-4,3′,5′), 7.46–7.55 (m, 5H, H-2,3,5,6,β), 7.88 (d, 2H, H-2′,6′, J = 8.0), 9.19 (s, 1H, *H*-Pyrazole), 12.31 (s, 1H, −COOH); Elemental analysis (%) of $C_{19}H_{16}N_2O_2$, calculated/found: C (74.99/74.98), H (5.32/5.30), N (9.21/9.20).

*3.1.2.3. 3-(3-(4-fluorophenyl)-1-phenyl-1H-pyrazol-4-yl)acrylic acid (**2c**).* Yield (%): 84; Appearance: White powder; m.p. 190–192 °C; IR (cm^{-1}): 1692 (C═O); ^{1}H NMR (400 MHz, DMSO): 6.39 (d, 1H, *H*-α, J = 16.0), 7.34–7.36 (m, 3H, H-4,3′,5′), 7.38 (d, 1H, *H*-β, J = 16.0), 7.46–7.52 (m, 2H, H-3,5), 7.62–7.66 (m, 2H, H-2′,6′), 7.88–7.90 (d, 2H, H-2,6, J = 8.0), 9.19 (s, 1H, *H*-Pyrazole), 12.31 (s, 1H, −COOH); Elemental analysis (%) of $C_{19}H_{16}N_2O_2$, calculated/found: C (70.12/70.11), H (4.25/4.24), N (9.09/9.10).

General procedure to synthesize benzohydrazide derivatives (**4a–i**)

Derivatives **3a–i** were synthesized in accordance with the reported methods [18–20]. Derivative **4i** was prepared using the method reported by Pakray and Castle [21].

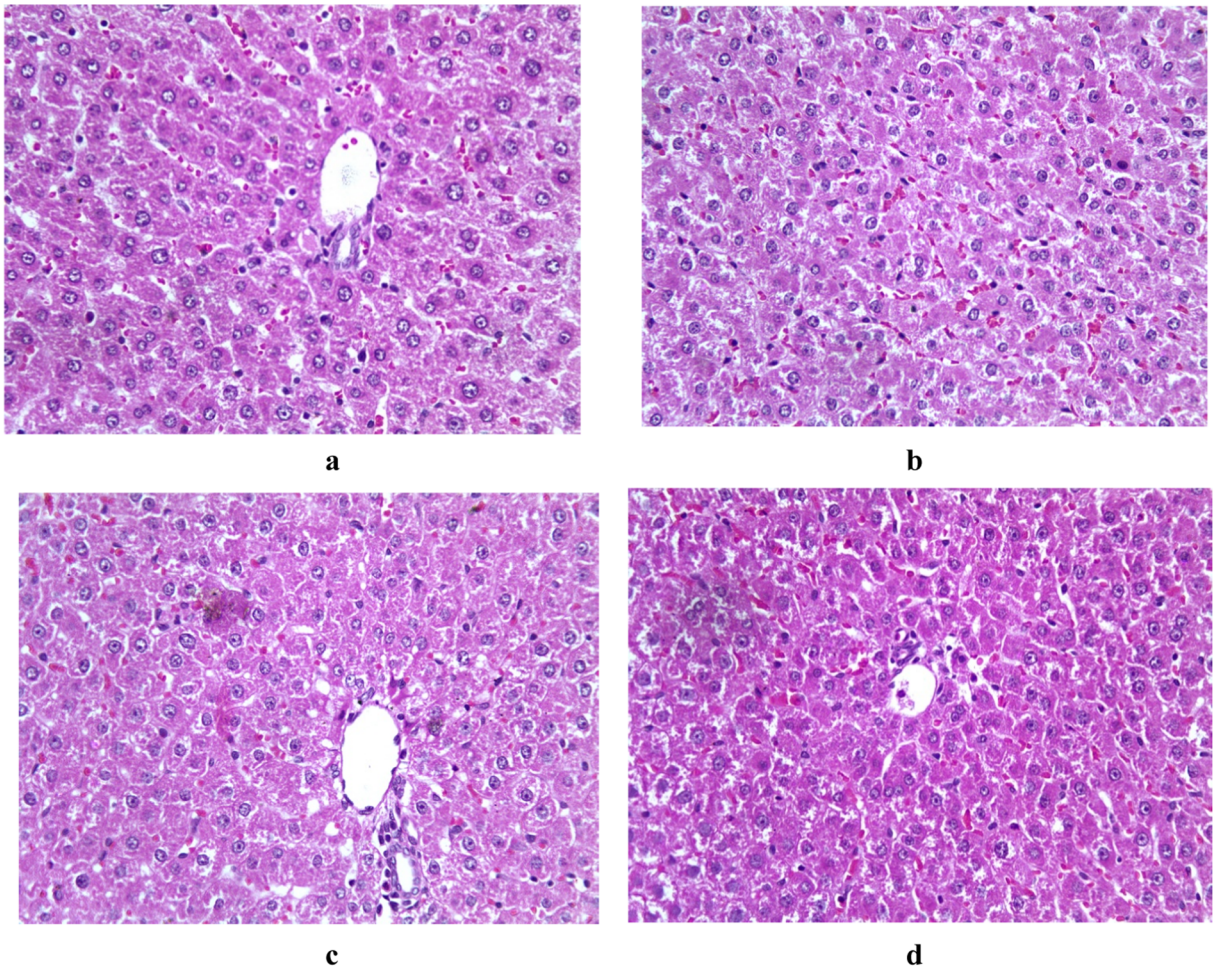

Fig. 10. (a) Liver architecture for control group (**b**) Liver architecture for test group (Compound **5f**) (**c**) Liver architecture for control group (**d**) Liver architecture for test group (Compound **5r**).

3.1.3. General procedure to synthesize 2-(2-(1,3-diphenyl-1H-pyrazol-4-yl) vinyl)-5-phenyl-1,3,4-oxadiazole derivatives (5a–v)

Scheme 1 was followed for synthesizing oxadiazole derivatives. Substitution for these derivatives is given in Table 4.

1,3,4-oxadiazole derivatives were prepared *via* direct coupling of the appropriately substituted hydrazide to the necessary acid derivative. To 10 mL of $POCl_3$, hydrazide (2 mmol) and acid (2 mmol) were added. The resulting reaction mixture was stirred at a temperature of 60–70 °C. Progress of the reaction was monitored using TLC. Following completion of the reaction, the reaction mixture was poured on crushed ice and neutralized with 10% sodium bicarbonate solution in water. Neutralized solution was filtered, washed with water and dried. The dried product was re-crystallized from methanol.

*3.1.3.1. 2-(2-(1,3-Diphenyl-1H-pyrazol-4-yl)vinyl)-5-(3,4,5-trimethoxyphenyl)-1,3,4-oxadiazole (**5a**).* Yield (%): 85; Appearance: Pale yellow solid; m.p. 216–220 °C; IR (cm^{-1}): 1626 (C═N), 1592 (C═C), 1243 (C—O—C); ^{1}H NMR (400 MHz, $CDCl_3$): 3.92 (s, 3H, OCH_3); 3.94 (s, 6H, 2 × OCH_3); 6.89 (d, 1H, *H*-α, *J* = 16.4 Hz); 7.29 (s, 2H, *H*-2″,6″); 7.34 (t, 1H, *H*-4, *J* = 16.4 Hz); 7.45–7.53 (m, 5H, *H*-3,5,3′,4′,5′); 7.62 (d, 1H, *H*-β, *J* = 16.4 Hz); 7.73 (d, 2H, *H*-2,6, *J* = 6.8 Hz); 7.79 (d, 2H, *H*-2′,6′, *J* = 8.0 Hz); 8.30 (s, 1H, *H*-Pyrazole); Mass *(m/z)*: 481 $[M+H]^+$; Elemental analysis (%) of $C_{28}H_{24}N_4O_4$, calculated/found: C (69.99/69.70), H (5.03/5.01), N (11.66/11.68)

*3.1.3.2. 2-(2-(1-Phenyl-3-(p-tolyl)-1H-pyrazol-4-yl)vinyl)-5-(3,4,5-trimethoxyphenyl)-1,3,4-oxadiazole (**5b**).* Yield (%): 87; Appearance: Pale yellow solid; m.p. 222–224 °C; IR (cm^{-1}): 1618 (C═N), 1596 (C═C), 1234 (C—O—C); ^{1}H NMR (400 MHz, $CDCl_3$): 2.44 (s, 3H, CH_3); 3.92 (s, 3H, OCH_3); 3.95 (s, 6H, 2XOCH_3); 6.88 (d, 1H, H-α, *J* = 16.4 Hz); 7.26–7.37 (m, 5H, H-4,3′,5′,2″,6″); 7.48 (t, 2H, H-3,5, *J* = 7.6 Hz); 7.57–7.65 (m, 3H, H-2,6,β); 7.78 (d, 2H, H-2′,6′, *J* = 8.0 Hz); 8.28 (s, 1H, *H*-Pyrazole); Mass *(m/z)*: 495 $[M+H]^+$; Elemental analysis (%) of $C_{29}H_{26}N_4O_4$, calculated/found: C (70.43/70.41), H (5.30/5.30), N (11.33/11.34)

*3.1.3.3. 2-(3,4-Dimethoxyphenyl)-5-(2-(1,3-diphenyl-1H-pyrazol-4-yl) vinyl)-1,3,4-oxadiazole (**5c**).* Yield (%): 88; Appearance: Yellow solid; m.p.158 °C; IR (cm^{-1}): 1614 (C═N), 1603 (C═C), 1248 (C—O—C); ^{1}H NMR (400 MHz, DMSO): 3.96 (s, 3H, OCH_3); 3.97 (s, 3H, OCH_3); 6.90 (d, 1H, *H*-α, *J* = 16.4 Hz); 6.95 (d, 1H, *H*-5″, *J* = 8.8 Hz); 7.34 (t, 1H, *H*-4, *J* = 6.8 Hz); 7.47–7.55 (m, 8H, *H*-2,3,5,6,3′,4′,5′,β); 7.68 (d, 2H, *H*-2′,6′, *J* = 7.2 Hz); 7.90 (d, 2H, *H*-2″,6″, *J* = 8.0 Hz); 9.23 (s, 1H, *H*-Pyrazole); Mass *(m/z)*: 451 $[M+H]^+$; Elemental analysis (%) of $C_{27}H_{22}N_4O_3$, calculated/found: C (71.99/71.98), H (4.92/4.93), N (12.44/12.46)

*3.1.3.4. 2-(3,4-Dimethoxyphenyl)-5-(2-(1-phenyl-3-(p-tolyl)-1H-pyrazol-4-yl)vinyl)-1,3,4-oxadiazole (**5d**).* Yield (%): 86; Appearance: Pale yellow solid; m.p. 164 °C; IR (cm^{-1}): 1618 (C═N), 1601 (C═C), 1244 (C—O—C); ^{1}H NMR (400 MHz, $CDCl_3$): 2.50 (s, 3H, CH_3); 3.86 (s, 3H, OCH_3); 3.87 (s, 3H, CH_3); 7.17 (d, 1H, *H*-5″, *J* = 8.8 Hz); 7.19 (d, 1H, *H*-α, *J* = 20.0 Hz); 7.39 (t, 1H, *H*-4, *J* = 7.2 Hz); 7.50–7.62 (m, 7H, *H*-3,5,3′,5′,2″,6″,β); 7.72 (d, 2H, *H*-2,6, *J* = 7.2 Hz); 7.94 (d, 2H, *H*-2′6′, *J* = 8.0 Hz); Mass *(m/z)*: 465 $[M^+ + H]$; Elemental analysis (%) of $C_{28}H_{24}N_4O_3$, calculated/found: C (72.40/72.41), H (5.21/5.19), N (12.06/12.07)

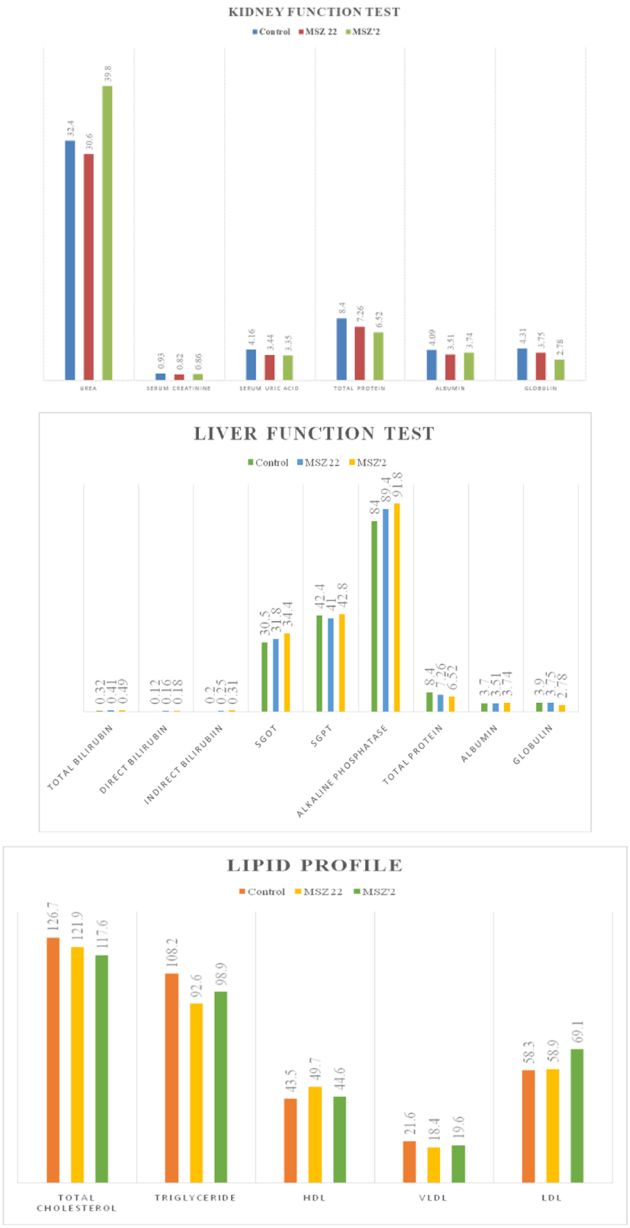

Fig. 11. Biochemical Estimation for Compounds **5f** and **5r** (**a**) Kidney Function Test (**b**) Liver Function Test (**c**) Lipid Profile.

3.1.3.5. 2-(3,4-Dimethoxyphenyl)-5-(2-(3-(4-fluorophenyl)-1-phenyl-1H-pyrazol-4-yl)vinyl)-1,3,4-oxadiazole ***(5e)***. Yield (%): 85; Appearance: Yellow solid; m.p. 212–214 °C; IR (cm^{-1}): 1632 (C═N), 1593 (C═C), 1239 (C–O–C); ^{1}H NMR (400 MHz, $CDCl_3$): 3.95 (s, 3H, OCH_3); 3.96 (s, 3H, OCH_3); 6.87 (d, 1H, *H*-α, *J* = 16.8 Hz); 6.94 (d, 1H, *H*-5″, *J* = 8.8 Hz); 7.18 (t, 2H, *H*-3′,5′, *J* = 8.8 Hz); 7.33 (t, 1H, *H*-4, *J* = 7.2 Hz); 7.46–7.71 (m, 7H, *H*-3,5,2′,6′,2″,6″,β); 7.76 (d, 2H, *H*-2,6, *J* = 8.4 Hz); 8.27 (s, 1H, *H*-Pyrazole); Mass *(m/z)*: 469 $[M+H]^+$; Elemental analysis (%) of $C_{27}H_{21}FN_4O_3$, calculated/found: C (69.22/69.23), H (4.52/4.50), N (11.96/11.97)

3.1.3.6. 2-(2-(1,3-Diphenyl-1H-pyrazol-4-yl)vinyl)-5-(furan-2-yl)-1,3,4-oxadiazole ***(5f)***. Yield (%): 89; Appearance: Yellow solid; m.p. 190–192 °C; IR (cm^{-1}): 1635 (C═N), 1590 (C═C), 1243 (C–O–C); ^{1}H NMR (400 MHz, $CDCl_3$): 66.60 (m, 1H, *H*-4″); 6.88 (d, 1H, *H*-α, *J* = 16.4 Hz); 7.17 (d, 1H, *H*-3″, *J* = 3.6 Hz); 7.34 (t, 1H, *H*-4, *J* = 7.2 Hz); 7.45–7.64 (m, 7H, *H*-3,5,3′,4′,5′, 5″, β); 7.71 (d, 2H, *H*-2,6, *J* = 7.2 Hz); 7.79 (d, 2H, *H*-2′,6′, *J* = 8.0 Hz); 8.30 (s, 1H, *H*-Pyrazole); Mass *(m/z)*: 381 $[M+H]^+$; Elemental analysis (%) of $C_{23}H_{16}N_4O_2$, calculated/found: C (72.62/72.63), H (4.24/4.22), N (14.73/14.74)

3.1.3.7. 2-(Furan-2-yl)-5-(2-(1-phenyl-3-(p-tolyl)-1H-pyrazol-4-yl)vinyl)-1,3,4-oxadiazole ***(5g)***. Yield (%): 84; Appearance: Yellow solid; m.p. 182–186 °C; IR (cm^{-1}): 1639 (C═N), 1596 (C═C), 1240 (C–O–C); ^{1}H NMR (400 MHz, $CDCl_3$): 2.45 (s, 3H, CH_3); 6.61 (m, 1H, *H*-4″); 6.87 (d, 1H, *H*-α, *J* = 16.4 Hz); 7.17 (d, 1H, *H*-3″, *J* = 3.2 Hz); 7.32–7.37 (m, 3H, *H*- 4,3′,5′); 7.48 (t, 2H, *H*-3,5, *J* = 8.0 Hz); 7.59–7.65 (m, 4H, *H*-2,6,5″, β); 7.78 (d, 2H, *H*-2′,6′, *J* = 8.0 Hz); 8.28 (s, 1H, *H*-Pyrazole); Mass *(m/z)*: 395 $[M+H]^+$; Elemental analysis (%) of $C_{24}H_{18}N_4O_2$, calculated/found: C (73.08/73.10), H (4.60/4.58), N (14.20/14.22)

3.1.3.8. 2-Benzyl-5-(2-(1,3-diphenyl-1H-pyrazol-4-yl)vinyl)-1,3,4-oxadiazole ***(5h)***. Yield (%): 89; Appearance: Yellow solid; m.p. 170–172 °C; IR (cm^{-1}): 1646 (C═N), 1591 (C═C), 1247 (C–O–C); ^{1}H NMR (400 MHz, $CDCl_3$): 5.26 (s, 2H, CH_2); 6.83 (d, 1H, H-α, *J* = 16.8 Hz); 7.03 (d, 2H, H-2″,6″, *J* = 6.4 Hz); 7.30–7.52 (m, 9H, H-3,4,5,3′,4′,5′,3″,4″,5″); 7.56 (d, 1H, H-β, *J* = 16.4 Hz); 7.67 (d, 2H, H-2,6, *J* = 7.6 Hz); 7.78 (d, 2H, H-2′,6′, *J* = 8.0 Hz); 8.28 (s, 1H, *H*-Pyrazole); Mass *(m/z)*: 405 $[M+H]^+$; Elemental analysis (%) of $C_{26}H_{20}N_4O$, calculated/found: C (77.21/77.23), H (4.98/4.97), N (13.85/13.85)

3.1.3.9. 2-Benzyl-5-(2-(1-phenyl-3-(p-tolyl)-1H-pyrazol-4-yl)vinyl)-1,3,4-oxadiazole ***(5i)***. Yield (%): 82; Appearance: pale yellow solid; m.p. 188 °C; IR (cm^{-1}): 1635 (C═N), 1589 (C═C), 1246 (C–O–C); ^{1}H NMR (400 MHz, $CDCl_3$): 2.43 (s, 3H, CH_3); 5.26 (s, 2H, CH_2); 6.82 (d, 1H, *H*-α, *J* = 16.4 Hz); 7.03 (d, 2H, *H*-2″,6″, *J* = 6.8 Hz); 7.30–7.36 (m, 5H, *H*-3,4,5,3′,5′); 7.47–7.60 (m, 6H, *H*-2,6,3″,5″,4″, β); 7.77 (d, 2H, *H*-2′,6′, *J* = 7.6 Hz); 8.26 (s, 1H, *H*-Pyrazole); Mass *(m/z)*: 419 $[M+H]^+$; Elemental analysis (%) of $C_{27}H_{22}N_4O$, calculated/found: C (77.49/77.52), H (5.30/5.32), N (13.39/13.40)

3.1.3.10. 2-(2-(1,3-Diphenyl-1H-pyrazol-4-yl)vinyl)-5-(4-methoxyphenyl)-1,3,4-oxadiazole ***(5j)***. Yield (%): 84; Appearance: Pale yellow solid; m.p.220 °C; IR (cm^{-1}):1633 (C═N), 1590 (C═C), 1244 (C–O–C); ^{1}H NMR (400 MHz, $CDCl_3$): 3.88 (s, 3H, OCH_3); 6.89 (d, 1H, *H*-α, *J* = 16.4 Hz); 6.99 (d, 2H, *H*-3″,5″, *J* = 8.8 Hz); 7.33 (t, 1H, *H*-4, *J* = 7.6 Hz); 7.45–7.55 (m, 5H, *H*-3,5,3′,4′,5′); 7.57 (d, 1H, *H*-β, *J* = *16.4* Hz); 7.72 (d, 2H, *H*-2,6, *J* = 7.2 Hz); 7.79 (d, 2H, *H*-2′,6′, *J* = 8.0 Hz); 7.99 (d, 2H, *H*-2″,6″, *J* = 8.8 Hz); 8.29 (s, 1H, *H*-Pyrazole); Mass *(m/z)*: 421 $[M+H]^+$; Elemental analysis (%) of $C_{26}H_{20}N_4O_2$, calculated/found: C (74.27/74.28), H (4.79/4.77), N (13.33/13.32)

3.1.3.11. 2-(4-Methoxyphenyl)-5-(2-(1-phenyl-3-(p-tolyl)-1H-pyrazol-4-yl)vinyl)-1,3,4-oxadiazole ***(5k)***. Yield (%): 80; Appearance: Yellow solid; m.p. 206–208 °C; IR (cm^{-1}):1639 (C═N), 1588 (C═C), 1240 (C–O–C); ^{1}H NMR (400 MHz, $CDCl_3$): 2.45 (s, 3H, CH_3); 3.88 (s, 3H, OCH_3); 6.88 (d, 1H, H-α, *J* = 16.4 Hz); 7.00 (d, 2H, H-3″,5″, *J* = 8.8 Hz); 7.33 (triplet merged with doublet, 3H, H-4,3′,5′, *J* = 6.8 Hz); 7.48 (t, 2H, H-3,5, *J* = 7.6 Hz); 7.56–7.63 (m, 3H, H-2,6,β); 7.78 (d, 2H, H-2′,6′, *J* = 8.0 Hz); 8.00 (d, 2H, H-2″,6″, *J* = 8.4 Hz); 8.28 (s, 1H, *H*-Pyrazole); Mass *(m/z)*: 435 $[M+H]^+$; Elemental analysis (%) of $C_{27}H_{22}N_4O_2$, calculated/found: C (74.64/74.66), H (5.10/5.13), N (12.89/12.88)

3.1.3.12. 2-(2,6-Dichlorophenyl)-5-(2-(1,3-diphenyl-1H-pyrazol-4-yl) vinyl)-1,3,4-oxadiazole ***(5l)***. Yield (%): 87; Appearance: Yellow solid; m.p. 194–196 °C; IR (cm^{-1}):; ^{1}H NMR (400 MHz, $CDCl_3$): 6.84 (d, 1H, H-α, *J* = 16.4 Hz); 7.34–7.40 (m, 2H, H-4,4″); 7.45–7.57 (m, 8H, H-3,5,3′,4′,5′,3″,5″,β); 7.69 (d, 2H, H-2,6, *J* = 6.4 Hz); 7.78 (d, 2H, H-2′,6′, *J* = 8.4 Hz); 8.29 (s, 1H, *H*-Pyrazole); Mass *(m/z)*: 459 $[M+H]^+$,

Table 4
List of synthesized derivatives in Scheme 1.

Comp.	R	X	Comp.	R	X	Comp.	R	X
5a	H	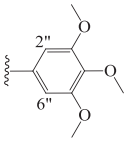	**5b**	4-CH_3	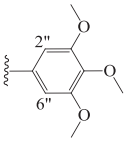	**5c**	H	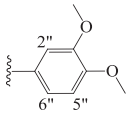
5d	4-CH_3	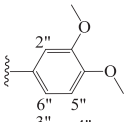	**5e**	4-F	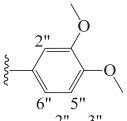	**5f**	H	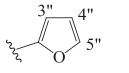
5g	4-CH_3	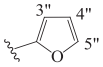	**5h**	H	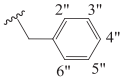	**5i**	4-CH_3	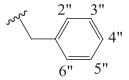
5j	H	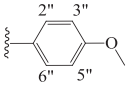	**5k**	4-CH_3	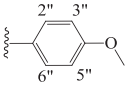	**5l**	H	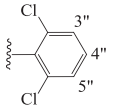
5m	4-CH_3	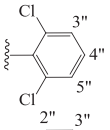	**5n**	H	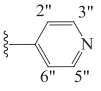	**5o**	4-CH_3	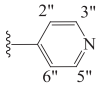
5p	H	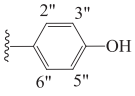	**5q**	4-CH_3	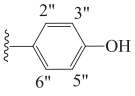	**5r**	4-CH_3	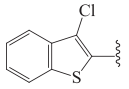

461 $[M-2+H]^+$, 463 $[M-4+H]^+$; Elemental analysis (%) of $C_{25}H_{16}Cl_2N_4O$, calculated/found: C (65.37/65.38), H (3.51/3.49), N (12.20/12.19)

*3.1.3.13. 2-(2,6-Dichlorophenyl)-5-(2-(1-phenyl-3-(p-tolyl)-1H-pyrazol-4-yl)vinyl)-1,3,4-oxadiazole (**5m**)*. Yield (%): 89; Appearance: Yellow solid; m.p. 210–212 °C; IR (cm^{-1}):1627 (C═N), 1595 (C═C), 1238 (C—O—C); ^1H NMR (400 MHz, $CDCl_3$): 2.44 (s, 3H, CH_3); 6.83 (d, 1H, *H*-α, *J* = 16.4 Hz); 7.29–7.36 (m, 5H, *H*-3,4,5,3′,5′); 7.48–7.52 (m, 3H, *H*-3″,4″,5″); 7.53 (d, 1H, *H*-β, *J* = 16.4 Hz); 7.59 (d, 2H, *H*-2,6, *J* = 8.0 Hz); 7.78 (d, 2H, *H*-2′,6′, *J* = 8.0 Hz); 8.26 (s, 1H, *H*-Pyrazole); Mass *(m/z)*:473 $[M+H]^+$; 475 $[M-2+H]^+$, 477 $[M-4+H]^+$; Elemental analysis (%) of $C_{26}H_{18}Cl_2N_4O$, calculated/found: C (65.97/65.98), H (3.83/3.85), N (11.84/11.84)

*3.1.3.14. 2-(2-(1,3-Diphenyl-1H-pyrazol-4-yl)vinyl)-5-(pyridin-4-yl)-1,3,4-oxadiazole (**5n**)*. Yield (%): 85; Appearance: Pale yellow solid; m.p. 200–202 °C; IR (cm^{-1}):1639 (C═N), 1593 (C═C), 1246 (C—O—C); ^1H NMR (400 MHz, $CDCl_3$): 6.91 (d, 1H, *H*-α, *J* = 16.4 Hz); 7.35 (t, 1H, *H*-4, *J* = 6.8 Hz); 7.47–7.56 (m, 5H, *H*-3,5,3′,4′,5′); 7.66 (d, 1H, *H*-β, *J* = 16.0 Hz); 7.71 (d, 2H, *H*-2,6, *J* = 7.2 Hz); 7.79 (d, 2H, *H*-2′,6′, *J* = 8.0 Hz); 7.92 (s, 2H, *H*-2″,6″); 8.33 (s, 1H, *H*-Pyrazole); 8.82 (s, 2H, *H*-3″,5″); ^{13}C NMR (100 MHz, $CDCl_3$): 108.32, 117.48, 118.93, 119.81, 125.67, 126.89, 128.28, 128.33, 128.41, 129.14, 130.21, 130.50, 131.77, 138.91, 150.35, 152.59, 161.55, 164.70; Mass *(m/z)*: 392 $[M+H]^+$; Elemental analysis (%) of $C_{24}H_{17}N_5O$, calculated/found: C (73.64/73.66), H (4.38/4.39), N (17.89/17.91)

*3.1.3.15. 2-(2-(1-Phenyl-3-(p-tolyl)-1H-pyrazol-4-yl)vinyl)-5-(pyridin-4-yl)-1,3,4-oxadiazole (**5o**)*. Yield (%): 81; Appearance: Yellow solid; m.p. 172–174 °C; IR (cm^{-1}): 1629 (C═N), 1596 (C═C), 1240 (C—O—C); ^1H NMR (400 MHz, $CDCl_3$): 2.46 (s, 3H, CH_3); 6.90 (d, 1H, *H*-α, *J* = 16.4 Hz); 7.30 (m, 3H, *H*-4,3′,5′); 7.49 (t, 2H, *H*-3,5, *J* = 8.0 Hz); 7.60 (d, 2H, *H*-2,6, *J* = 8.0 Hz); 7.67 (d, 1H, *H*-β, *J* = 16.8 Hz); 7.79 (d, 2H, *H*-2′,6′, *J* = 7.6 Hz); 7.92 (d, 2H, *H*-2″,6″); 8.31 (s, 1H, *H*-Pyrazole); 8.82 (s, 2H, *H*-3″,5″); Mass *(m/z)*: 406 $[M+H]^+$; Elemental analysis (%) of $C_{25}H_{19}N_5O$, calculated/found: C (74.06/74.09), H (4.72/4.70), N (17.27/17.29)

*3.1.3.16. 4-(5-(2-(1,3-Diphenyl-1H-pyrazol-4-yl)vinyl)-1,3,4-oxadiazol-2-yl)phenol (**5p**)*. Yield (%): 87; Appearance: Yellow solid; m.p. 172–174 °C; IR (cm^{-1}): 1631 (C═N), 1594 (C═C), 1237 (C—O—C), 3315 (OH); ^1H NMR (400 MHz, $CDCl_3$): 6.93 (d, 2H, *H*-3″,5″, *J* = 8.4 Hz); 7.16 (d, 1H, *H*-α, *J* = 16.4 Hz); 7.36 (t, 1H, *H*-4, *J* = 7.2 Hz); 7.49–7.58 (m, 6H, *H*-β, 3,5,3′,4′,5′); 7.69 (d, 2H, *H*-2,6, *J* = 7.2 Hz); 7.83 (d, 2H, *H*-2′,6′, *J* = 8.4 Hz); 7.91 (d, 2H, *H*-2″,6″, *J* = 7.6 Hz); 10.27 (bs, 1H, OH); Mass *(m/z)*: 407 $[M+H]^+$; Elemental analysis (%) of $C_{25}H_{18}N_4O_2$, calculated/found: C (73.88/70.91), H (4.46/4.44), N (13.78/13.78)

*3.1.3.17. 4-(5-(2-(1-Phenyl-3-(p-tolyl)-1H-pyrazol-4-yl)vinyl)-1,3,4-oxadiazol-2-yl)phenol (**5q**)*. Yield (%): 80; Appearance: Yellow solid; m.p. 190–194 °C; IR (cm^{-1}):1635 (C═N), 1591 (C═C), 1247 (C—O—C), 3328 (OH); ^1H NMR (400 MHz, $CDCl_3$): 2.49 (s, 3H, CH_3); 7.14–7.20 (m, 3H, *H*-3″,5″,α); 7.31–7.38 (m, 5H, *H*-3,4,5,3′,5′); 7.49–7.59 (m,3H, *H*-2,6,β); 7.82 (d, 2H, *H*-2′,6′, *J* = 8.4 Hz); 7.90 (d, 2H, *H*-2″,6″, *J* = 8.0 Hz); 9.25 (s, 1H, *H*-Pyrazole); 9.27 (bs, 1H, OH); Mass *(m/z)*: 421 $[M+H]^+$; Elemental analysis (%) of $C_{26}H_{20}N_4O_2$, calculated/found: C (74.27/74.27), H (4.79/4.82), N (13.33/13.35)

*3.1.3.18. 2-(3-chlorobenzo[b]thiophen-2-yl)-5-(2-(1-phenyl-3-(p-tolyl)-1H-pyrazol-4-yl)vinyl)-1,3,4-oxadiazole (**5r**)*. Yield (%): 80; Appearance: Yellow solid; m.p. 188 °C; IR (cm^{-1}): 1638 (C═N), 1595 (C═C), 1242 (C—O—C); ^1H NMR (400 MHz, $CDCl_3$): 2.48 (s, 3H, CH_3); 6.94 (d, 1H, *H*-α, *J* = 16.4 Hz); 7.35 (t, 3H, *H*-4,3′,5′, *J* = 8.0 Hz); 7.51–7.57 (m, 4H, *H*-3,5,4″,7″); 7.65 (d, 2H, *H*-2,6, *J* = 8.0 Hz); 7.75 (d, 1H, *H*-β, *J* = 16.0 Hz); 7.82 (d, 2H, *H*-2′,6′, *J* = 7.6 Hz); 7.88–7.91 (m, 1H, *H*-6″); 7.99 (m, 1H, *H*-5″); 8.34 (s, 1H, *H*-Pyrazole); Mass *(m/z)*: 495 $[M+H]^+$; 497 $[M-2+H]^+$; Elemental analysis (%) of $C_{26}H_{20}N_4O_2$, calculated/found: C (67.94/67.95), H (3.87/3.85), N (11.32/11.33)

3.2. Pharmacological activity

3.2.1. Antimalarial activity

3.2.1.1. Schizont maturation inhibition assay. Synchronization of culture of chloroquine sensitive 3D7 strain of *P. falciparum* was done using 5% aqueous solution of sorbitol. All stages except rings were degenerated. With this, a collection of parasites of similar stage was obtained. Centrifugation for 5 min at 1500 rpm was done for removing degenerated stages. Supernatant was discarded and the pellet was washed twice using incomplete media.

Adjustment of parasitemia to about 1% for assay was done by dilution with fresh washed RBCs. Synthesized compounds that were to be assessed for antimalarial efficacy were dissolved in 100 µL of DMSO. Control well also received the same concentration of DMSO. Dilution of the stock solution was done in RPMI-1640 for obtaining different concentrations. Chloroquine served as the standard for carrying out this study.

Testing was done in 96 well plate using chloroquine sensitive isolates. Prepared concentrations of the compounds were dispensed in 96 well plate using chloroquine sensitive isolates. Drug was not added to the first well of all the rows and was considered as the control well. Synchronized parasites were inoculated in all the wells, even the control one to get a final concentration of 5% haematocrit. Same protocol was adopted to determine the efficacy of compounds against chloroquine resistant strain of *P. falciparum* (RKL 9).

Depending on the maturation of schizont, these plates were incubated at 37 °C in gas mixture containing 90% N_2, 5% CO_2 and 5% O_2 for a period of 24–30 h. Following confirmation of schizont maturation, smears were prepared from all the wells. Staining of these smears was done using JSB II and JSB I stains. The dried slides were observed under power of the Nikon Eclipse E200 microscope. Total number of schizonts (3 or more merozoites) per 200 asexual parasites was counted. IC_{50} value for each compound was calculated from total number of schizonts using HN-NonLin Regression analysis (malaria.farch.net). Active compounds of the series were further tested against chloroquine resistant strain, RKL9 [22]. Cytotoxicity studies for the synthesized compounds were carried out using *Vero* cell line. Mossman method with certain modifications was adopted for performing *in vitro* cytotoxicity assay [23]. Cells with different dilutions of compounds were incubated for a period of 72 h using MTT reagent. Using the formula, CC_{50}/IC_{50}, SI of the compounds was calculated. Here, CC_{50} refers to cytotoxic concentration, required to bring about death of 50% of the fibroblast cells. Values for SI of compounds are given in Table 2. For these compounds, resistance index (RI) was determined by dividing IC_{50}:*Pf*RKL9/IC_{50}:*Pf*3D7.

3.2.1.2. In vitro Falcipain-2 assay. Diluted, soluble *P. falciparum* Falcipain-2 (30 nM) was incubated at room temperature in 100 mM sodium acetate, pH 5.5, 10 mM DTT, along with different concentrations of compounds to be tested or the standard agent, E64 for a duration of 10 min. After incubation for the stipulated time period, a fluorescent substrate, Cbz-Phe-Arg-AMC was added to a final concentration of 25 µM. Intensity of fluorescence (excitation: 355 nm, emission: 460 nm) was determined for 10 min at room temperature using SynergyTM 4 Multi-Mode Microplate Reader (BioTek). Following formula was used for determining the inhibition rate (%).

$$\%\ \text{Inhibition} = [1 - (F\ \text{test}/F\ \text{control})] \times 100$$

Here, *F* test refers to the fluorescence intensity of test compound whereas *F* control is the fluorescence intensity of standard agent, E64. All the values are mean values of triplicate independent determinations and deviations are < 10% of the mean value. IC_{50} values for falcipain-2 were determined for compounds exhibiting 50% or more enzyme inhibition at a dose of 25 µM.

3.2.1.3. Molecular docking studies. Molecular docking studies were performed for antimalarial compounds. Catalytic domain for falcipain-2 (PDB ID: **1YVB**) was obtained from protein data bank. Protein preparation wizard [24], available in Schrödinger suite 2016-1 was used for preparing protein. Crystallographic water molecules *i.e.* without 3*H* bonds were deleted and hydrogen bonds corresponding to pH 7 were added considering the appropriate ionization states for both acidic and basic amino acid residues. For energy minimization of the crystal structure, OPLS_2005 force field was used. Site map was run to identify the active site of the Falcipain-2 enzyme. Selection amongst the generated sites was made on the basis of site score and further, centroid was taken for further grid generation. Active site was defined with a radius of 16 Å around the centroid. For docking, low energy conformations of all the compounds were docked into the catalytic domain of both enzymes using Grid based Ligand Docking with Energetics (Glide v7.0, Schrödinger 2016-1) in standard precision (SP) mode in the absence of any constraint.

3.2.2. Antileishmanial activity

For carrying out antileishmanial activity, fetal bovine serum (FBS) was obtained from Gibco-BRL, DMSO from SRL and methanol from Merck. All the other chemicals required in the study were procured from Sigma-Aldrich, unless mentioned.

L. donovani parasites, strain MHOM/IN/83/AG83, were maintained *in vivo* in BALB/c mice. Culturing of promastigotes was carried out in M199 medium supplemented with 10% hematin activated FBS, penicillin G sodium (100 U/mL) and streptomycin sulfate (100 µg/mL) at a temperature of 22 °C. Sub-culturing was done every 72 h in the same medium at a mean density of 2×10^6 cells/mL [25]. Cell line, RAW264.7 was grown at 37 °C in RPMI 1640 medium (pH 7.4) supplemented with 10% heat-inactivated FBS for 48–72 h in 5% CO_2 and sub-cultured in fresh RPMI 1640 medium at a mean density of 2×10^5 cells/mL.

Screening of compounds was performed against the promastigote stage of *L. donovani in vitro*. Incubation of promastigotes of *L. donovani* in M199 medium was done for a period of 48 h at a temperature of 22°C with each compound at a concentration of 100 µg/mL. Pentamidine served as the standard drug for the whole study while 0.2% DMSO was taken as the solvent control. Parasites with media alone were taken as control. Viability of parasites was determined microscopically after a period of 48 h [26].

For determination of IC_{50} values, promastigotes (2×10^6 cells/mL) were incubated for 48 h at a temperature of 22 °C without or with serial two fold dilutions of **5a, 5c** and **5r** starting from 100 µg/mL. MTT assay was adopted for determining mean percent (%) viability. IC_{50}, inhibitory concentration responsible for 50% reduction in promastigote growth was graphically extrapolated by plotting percent (%) viability versus drug concentration. DMSO was taken as the negative control while Pentamidine served as the reference drug [27].

3.3. Acute oral toxicity studies

Acute oral toxicity testing for compounds **5f** and **5r** was carried out in accordance with OECD guideline for testing chemicals. Two groups *i.e.* control and test comprising of three Wistar rats each (female) were made. Each animal selected for inclusion into each group was between 8 and 12 weeks old. Animals were initially housed in the Central Animal Housing Facility of Jamia Hamdard. Rats were kept at a temperature of 22 ± 3 °C. Relative humidity was maintained between 40 and 50%. They were provided with 12 h cycle each of light and dark. They were fed with conventional laboratory diets and unlimited availability of drinking water.

Five days prior to our experimentation, animals were shifted to the laboratory where experiments were to be performed. This was done to permit acclimatization to the laboratory conditions.

For dosing, our most active compounds (**5f** and **5r**) were suspended in carboxy methyl cellulose at a concentration of 300 mg/Kg. Prepared doses were administered to rats using an oral gavage. Prior to dosing,

supply of food was withheld for an overnight period. However, an uninterrupted supply of water was there.

Dosed animals were observed initially during first 30 min, periodically during first 24 h and thereafter for a window of 14 days. During the course of observation, all the signs of toxicity and vital parameters were observed and recorded. On 15th day, all the animals were sacrificed, liver was removed and observed for histopathological changes. Blood was collected and sent for biochemical examination.

4. Structure activity correlation

4.1. Antimalarial activity

Results obtained for antimalarial activity of the synthesized compounds were keenly observed. These results further strengthened the previous hypothesis developed on the basis of results of the already reported series of compounds. Previously, compound **6v** having an unsubstituted acetophenone part along with the presence of a heteroaromatic ring (indole), showed most promising antimalarial effects [12].

In the present series of compounds, compound **5f** bearing an unsubstituted acetophenone part and a heteroaromatic ring (furan) emerged as the most potent antimalarial agent. In both the cases, heteroaromatic ring is directly linked to oxadiazole moiety. Results for both the compounds were found to be comparable to each other. Compound **6v** (previous paper) elicited an IC_{50} value of 0.245 μg/mL against 3D7 strain of *P. falciparum* while **5f** showed an IC_{50} value of 0.248 μg/mL.

5. Conclusion

Prevailing conditions of resistance to the available antimalarial agents and toxicity profile associated with clinically used antileishmanial agents demand assiduous efforts towards development of novel and safer therapeutic options. Present work represents an extension of the previously reported work. This covers synthesis, spectral characterization and pharmacological evaluation of 1,3,4-oxadiazole based compounds. Amongst the prepared derivatives, compound **5f** emerged as the most potent antimalarial agent with appreciable activity against Falcipain-2 enzyme. Probable mode of action of compound **5f** was ascertained using docking studies and enzyme assay. On comparing these results with the previously reported results, close affinity was observed. On the whole, it was inferred that previously reported hypothesis "presence of heteroaromatic ring linked to 1,3,4-oxadiazole moiety favored antimalarial activity" was further strengthened by the results obtained for compounds of the present series. This time, in addition with antimalarial activity, antileishmanial effects were also assessed. Compound **5r** showed promising results against the promastigote stage of parasite. Further, results of acute oral toxicity studies suggested that compounds **5f** and **5r** could be considered safe as no signs of toxicity were observed in histological studies and biochemical evaluation.

Acknowledgements

Authors are thankful to Jamia Hamdard, New Delhi and National Institute of Malaria Research, New Delhi. One of the authors is thankful to University Grants Commission, New Delhi for providing financial assistance.

Conflict of interest

Authors declare no conflict of interest.

References

[1] S. Sahu, S.K. Ghosh, J. Kalita, M. Dutta, H.R. Bhat, Design, synthesis and antimalarial screening of some hybrid 4-aminoquinoline-triazine derivatives against *pf*-DHFR-TS, Exp. Parasitol. 163 (2016) 38–45.
[2] World Malaria Report, 2016.
[3] G. Verma, G. Chashoo, A. Ali, M.F. Khan, W. Akhtar, I. Ali, M. Akhtar, M.M. Alam, M. Shaquiquzzaman, Synthesis of pyrazole acrylic acid based oxadiazoles and amide derivatives as antimalarial and anticancer agents, Bioorg. Chem. 77 (2018) 106–124.
[4] A. Upadhyay, P. Kushwaha, S. Gupta, R.P. Dodda, K. Ramalingam, R. Kant, N. Goyal, K.V. Sashidhara, Synthesis and evaluation of novel triazolyl quinoline derivatives as potential antileishmanial agents, Eur. J. Med. Chem. 154 (2018) 172–181.
[5] M. Yousuf, D. Mukherjee, S. Dey, S. Chatterjee, A. Pal, B. Sarkar, C. Pal, S. Adhikari, Synthesis and biological evaluation of polyhydroxylated oxindole derivatives as potential antileishmanial agent, Bioorg. Med. Chem. Lett. 28 (2018) 1056–1063.
[6] N. Arshad, J. Hashim, Irfanullah, M.A. Minhas, J. Aslam, T. Ashraf, S.Z. Hamid, T. Iqbal, S. Javed, New series of 3,5-Disubstituted tetrahydro-2H-1,3,5-thiadiazine thione (THTT) derivatives: synthesis and potent antileishmanial activity, Bioorg. Med. Chem. Lett. 28 (2018) 3251–3254.
[7] M.S. dos Santos, M.L.V. Oliveira, A.M.R. Bernardino, R.M. de Leo, V.F. Amaral, F.T. de Carvalho, L.L. Leon, M.M. Canto-Cavalheiro, Synthesis and antileishmanial evaluation of 1-aryl-4-(4,5-dihydro-1*H*-imidazol-2-yl)-1*H*-pyrazole derivatives, Bioorg. Med. Chem. Lett. 21 (2011) 7451–7454.
[8] J.V. Faria, M.S. dos Santos, A.M.R. Bernardino, K.M. Becker, G.M.C. Machado, R.F. Rodrigues, M.M. Canto-Cavalheiro, I.L. Leon, Synthesis and activity of novel tetrazole compounds and their pyraozle-4-carbonitrile precursors against *Leishmania spp*, Bioorg. Med. Chem. Lett. 23 (2013) 6310–6312.
[9] A. Taha, A.A. Bekhit, Y. Seid, Screening of some pyrazole derivatives as promising antileishmanial agent, African J. Pharm. Pharmacol. 11 (2017) 32–37.
[10] A.A. Bekhit, A.M.M. Hassan, H.A.A.E. Razik, M.M.M. El-Miligy, E.J. El-Agroudy, A.E.D.A. Bekhit, New heterocyclic hybrids of pyrazole and its bioisosteres: design, synthesis and biological evaluation as dual acting antimalarial-antileishmanial agents, Eur. J. Med. Chem. 94 (2015) 30–44.
[11] M. Taha, N.H. Ismail, S. Imran, E.H. Anouar, M. Selvaraj, W. Jamil, M. Ali, S.M. Kashif, F. Rahim, K.M. Khan, M.I. Adenan, Synthesis and molecular modeling studies of phenyl linked oxadiazole-phenylhydrazone hybrids as potent antileishmanial agents, Eur. J. Med. Chem. 126 (2017) 1021–1033.
[12] M. Taha, N.H. Ismail, M. Ali, U. Rashid, S. Imran, N. Uddin, K.M. Khan, Molecular hybridization conceded exceptionally potent quinolinyl-oxadiazole hybrids through phenyl linked thiosemicarbazide antileishmanial scaffolds: *In silico* validation and SAR studies, Bioorg. Chem. 71 (2017) 192–200.
[13] M.P. Reddy, G.S.K. Rao, Applications of the Vilsmeier reaction, 13, Vilsmeier approach to polycyclic aromatic hydrocarbons, J. Org. Chem. 46 (1981) 5371–5733.
[14] A.M.A.D. Souza, V.L.D.M. Guarda, L.F.C.D.C. Leite, J.M.B. Filho, M.D.C.A.D. Lima, S.L.G.I.D.R. Pitta, On application of knoevenagel condensation for the synthesis of benzylidene benzothiazine compounds and structural study, Quim Nova 29 (2006) 1106–1109.
[15] K.E. Kolb, K.W. Field, P.F. Schatz, One step synthesis of cinnamic acids using malonic acid: the Verley-Doebner modification of the knoevenagel condensation, J. Chem. Edu. A304.
[16] M.J. Naim, M.J. Alam, F. Nawaz, V.G.M. Naidu, S. Aghaz, M. Sahu, N. Siddiqui, O. Alam, Synthesis, molecular docking and anti-diabetic evaluation of 2,4-thiazolidinedione based amide derivatives, Bioorg. Chem. 73 (2017) 24–36.
[17] J.J. Vora, S.B. Vasava, K.C. Parmar, S.K. Chauhan, S.S. Sharma, Synthesis, spectral and microbial studies of some novel Schiff base derivatives of 4-Methylpyridin-2-amine, J. Chem. 6 (2009) 1205–1210.
[18] Z. Chen, W. Xu, K. Liu, S. Yang, H. Fan, P.S. Bhadury, D.Y. Hu, Y. Zhang, Synthesis and antiviral activity of 5-(4-Chlorophenyl)-1,3,4-thiadiazole sulfonamides, Molecules. 15 (2010) 9046–9056.
[19] J.R. Maxwell, D.A. Wasdahl, A.C. Wolfson, V.I. Stenberg, Synthesis of 5-Aryl-2Htetrazoles,5-Aryl-2H-tetrazole-2-acetic acids, and [(4-Phenyl-5-aryl-4*H*-1,2,4-triazol-3-yl)thio]acetic acids as possible superoxide scavengers and anti-inflammatory agents, J. Med. Chem. 27 (1984) 1565–1570.
[20] A. Rehman, A. Fatima, M.A. Abbasi, S. Rasool, A. Malik, M. Ashraf, I. Ahmad, S.A. Ejaz, Synthesis of new *N*-(5-chloro-2-methoxyphenyl)-4-(5-substituted-1,3,4-oxadiazol-2-ylthio)butanamide derivatives as suitable lipoxygenase inhibitors, J. Saudi Chem. Soc. 20 (2016) S488–S494.
[21] S. Pakray, R.N. Castle, The synthesis of Dimethoxy[1]benzothieno[2,3-*c*]quinolines, J. Heterocyclic Chem. 23 (1986) 1571–1577.
[22] A.K. Pandey, S. Sharma, M. Pandey, M.M. Alam, M. Shaquiquzzaman, M. Akhter, 4,5-Dihydrooxazole-pyrazoline hybrids: synthesis and their evaluation as potential antimalarial agents, Eur. J. Med. Chem. 123 (2016) 476–486.
[23] T. Mosmann, Rapid colorimetric assay for cellular growth and survival: application to proliferation and cytotoxicity assays, J. Immunol. Methods 65 (1983) 55–63.
[24] G.M. Sastry, M. Adzhigirey, T. Day, R. Annabhimoju, W. Sherman, Protein andligand preparation: parameters, protocols and influence on virtual screening enrichments, J. Comput. Aided Mol. Des. 27 (2013) 221–234.
[25] F. Afrin, T. Dey, K. Anam, N. Ali, Leishmanicidal activity of stearylamine-bearing liposomes *in vitro*, J. Parasitol. 87 (2001) 188–193.
[26] S. Shafi, F. Afrin, M. Islamuddin, G. Chouhan, I. Ali, F. Naaz, K. Sharma, M.S. Zaman, β-nitrostyrenes as potential anti-leishmanial agents, Front. Microbiol. 7 (2016) 1–16.
[27] M. Islamuddin, D. Sahal, F. Afrin, Apoptosis-like death in *Leishmania donovani* promastigotes induced by eugenol-rich oil of *Syzygium aromaticum*, J. Medical Microbiol. 63 (2014) 74–85.